Nuclear Engineering and Technology 55 (2023) 1665–1670

Contents lists available at ScienceDirect

Nuclear Engineering and Technology

journal homepage: www.elsevier.com/locate/net

Original Article

On the cyclic change in the dynamics of the IBR-2M pulsed reactor

Yu.N. Pepelyshev, Sumkhuu Davaasuren*

Frank Laboratory of Neutron Physics, Joint Institute for Nuclear Research, Dubna, Russia

ARTICLE INFO

Article history:
Received 8 August 2022
Received in revised form
2 January 2023
Accepted 3 January 2023
Available online 5 January 2023

Keywords:
IBR-2M
Pulsed reactor
Power feedback
Control rod
Reactor stability

ABSTRACT

It is shown that in the IBR-2M reactor by the end of the reactor cycle, changes in dynamics are observed associated with a strong weakening of the fast power feedback (PF), as a result of which the reactor becomes oscillatorily unstable. After each week of zero-power operation the negative changes in reactor dynamics disappear and the stability of the reactor is restored. Thus, the reactor undergoes cyclic changes in the oscillatory instability. The correlation between of a fast PF and a slow PF is experimentally observed, which makes it possible to almost completely eliminate the cyclic component of instability by changing the control mode of rods of the control system.

1. Introduction

The IBR-2M pulsed reactor of periodic operation has been operating since 2012 at JINR (Dubna) at a pulse frequency of 5 Hz and an average power of 2 MW. The reactor's operating mode is organized in the so-called cyclic mode: two weeks at rated power, followed by a break for a week at zero power. In this cyclic mode, the dynamics of the IBR-2M also experience cyclic changes. These changes manifest themselves in the fact that the stability of the reactor deteriorates by the end of the cycle, and is restored by the beginning of the next cycle. Instabilities manifest themselves as an increase in the amplitude of low-frequency (with a period of 10 s) pulse energy fluctuations. The cyclic changes in dynamics and the corresponding cyclic change in oscillatory instability of the pulsed reactor give valuable insight in IBR-2M's dynamics. Given the operational importance of safety and control, we conducted a study of the auto-oscillatory regime and its dependence on the cyclic operating regime of the reactor. Based on the developed model of the IBR-2M dynamics and experimental data on the parameters of fast power feedback, the authors evaluated the structure of the oscillatory instability of the reactor and identified a set of factors affecting stability. Ways of escaping from cyclic instability are shown and directions for further research are given.

2. Introduction to problem

Literature sources from the 1950s and 1960s describe cases of auto-oscillation in continuous reactors. Documented cases indicate auto-oscillations possibly leading to even core meltdown [1]. In pulsed batch reactors, auto-oscillatory effects should appear much stronger than in stationary reactors. Firstly because of the higher sensitivity of the pulse reactor to changes in reactivity, and secondly the “pulses” itself, under certain conditions, can resonantly amplify the auto-oscillations. The IBR-2M is characterized by the following. As the energy output increases, the fast power feedback (PF) weakens, and low-frequency pulse energy fluctuations occur in the reactor at some stage of operation [2]. The power feedback for the IBR-2M, whose time constants are less than 2 min, is considered to be fast feedback. Although some body of experimental evidence exists, the nature of auto-oscillations in pulsed reactors is still not entirely understood. For example, despite the differences, the manifestations of auto-oscillations for both reactors (IBR-2 and IBR-2M) have some common patterns. The main one is that in the process of the growth of the total energy output (from the beginning of the campaign) there is an increase (accumulation) of instability [2]. It can be assumed that the cumulative effect of instability is associated with degradation processes occurring in the core or in its immediate vicinity.

There is another effect of oscillatory instability - cyclical one. The cyclic effect appeared more clearly on the IBR-2M. It consists in the following: in a short period of time at a fairly low energy output (~20–30 MW·day) the reactor enters an oscillatory state. In

* Corresponding author.
E-mail address: sumkhuu0322@gmail.com (S. Davaasuren).

https://doi.org/10.1016/j.net.2023.01.004

practically two weeks of operation, a reactor can go from stable to unstable state. After the reactor stops, the negative changes in the dynamics accumulated over the cycle disappear, and the oscillatory instability intensifies again in the next cycle. This effect can be called cyclic, because it repeats from cycle to cycle. To understand the above, Fig. 1 shows a scheme of attenuation of fast PF during operation of the IBR-2M. Fig. 1 shows the variation of the accumulated k''_T and cyclic k'_T components of the fast PF transfer coefficient. It can be seen that over time the reactor can approach the region of instability marked in Fig. 1 by the $k_T = k''_T + k'_T = -2\,\beta_p$/MW coefficient**.**

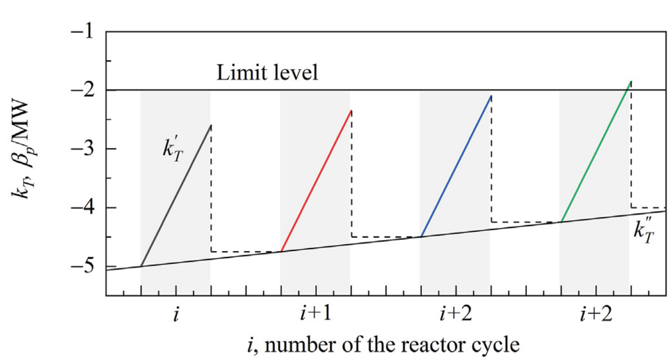

Fig. 1. Scheme of attenuation of fast PF during operation of the IBR-2M: k_T – total transfer coefficient of fast PF (β_p/MW), k'_T, k''_T – cyclic and accumulated components of k_T, respectively.

3. Design and operating principle of the IBR-2M pulsed reactor

Let us briefly note the features of the IBR-2M reactor. The core has the shape of a vertical hexagonal prism (Fig. 2). All but one of the prism faces are surrounded by reflectors that can move vertically. These reflectors act as control and protection organs: compensating organs (CO_1, CO_2), automatic regulator (AR), intermediate regulator (IR) and emergency protection (EP_1, EP_2), which ensures the termination of the chain reaction. Compensating organs compensate for fuel burnup and negative feedback reactivity due to reactor heating up. The automatic regulator maintains the power at the set level. The intermediate regulator is switched on by the operator to compensate for slow reactivity drifts. The movable reflector (MR), which consists of two steel blades, runs past the free face. The blades rotate in opposite directions at different speeds in a helium-filled casing. The speed of the main moving reflector is 600 rpm, the additional one is 300 rpm. When the blades pass the core at the same time, a reactivity pulse is created. The reactor is in a supercritical state on prompt neutrons for ~400 μs? During this time there is a rapid increase in power. When the blades move away from the core, the reactor becomes deeply subcritical, the reactor power drops rapidly. The efficiency of the moving reflector Δk_{MR} is very high $\Delta k_{MR} = 0.03$, i.e. 3%. As a result, the reactor generates power pulses of ~200 μs duration with a period of 0.2 s. 92% of the energy generated by the reactor is released in pulses, and 8% is released between pulses.

4. Brief description of the dynamics model of the IBR-2M

To study the dynamics of the IBR-2M, a mathematical model of the reactor was created [3–7]. With the help of this model it is possible to analyze the pulse energy transients and the frequency transfer characteristics of the reactor and use them to estimate the stability margin.

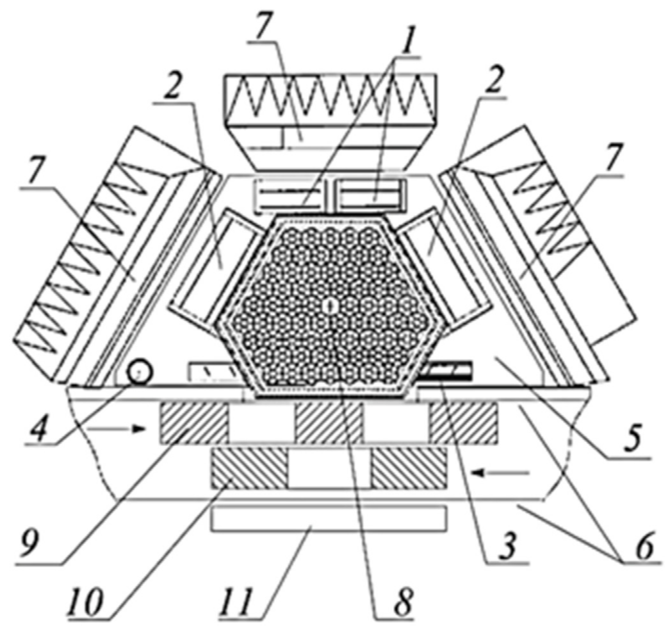

Fig. 2. Cross-sectional view of the IBR–2M core: *1* – emergency protection rods; *2* – compensation rods 1, 2; *3* – intermediate regulator; *4* – automatic regulator; *5* – stationary reflector; *6* – movable reflector supports; *7* – grooved water moderators; *8* – external neutron source; *9* – main movable reflector; *10* – auxiliary movable reflector; *11* – flat water moderator.

The model is based on a modular structure with blocks of kinetics, perturbing reactivity, automatic regulation and power feedback block [3–5] (Fig. 3).

The perturbing reactivity block includes data on the differential efficiency of all controls, as well as on various simulated reactivity change processes. The kinetics block corresponds to the system of equations of the pulsed reactor derived from the equations of the one-point kinetics model [3,4]. The automatic regulation unit is represented by a filter unit and a regulation unit [5]. The nonlinear kinetics system in the model is represented in the linearized form of discrete frequency transfer functions of the reactor. Since the reactivity deviations in our experiment were rather small, a linearized model could be used to estimate the stability margin. For large reactivity deviations, the linearized model cannot be used.

The linearized equations of kinetics and PF of the IBR-2M correspond to the structural scheme shown in Fig. 4. The parameters of the fast PF (transfer coefficients and time constants) were determined experimentally. The slow PF effects are sufficiently compensated by the automatic power stabilization system and are not taken into account in the IBR-2M stability model. The Nyquist frequency criterion was used to estimate the stability margin.

Expressions for the frequency discrete transfer functions of kinetics ($W^*_S(j\bar{\omega}), W^*_E(j\bar{\omega})$) and PF ($W^*_{T\Delta E}(j\bar{\omega})$) in general are as follows:

$$W^*_{RT}(j\bar{\omega}) = \frac{\Delta e^*_p(j\bar{\omega})}{\Delta r^*(j\bar{\omega})} = \frac{1}{1 + W^*_E(j\bar{\omega})\left[E^0 W^*_{T\Delta E}(j\bar{\omega}) - W^*_S(j\bar{\omega})\right]}, \tag{1}$$

where $W^*_S(j\bar{\omega})$, $W^*_E(j\bar{\omega})$ and $W^*_{T\Delta E}(j\bar{\omega})$ are calculated by the following formulas

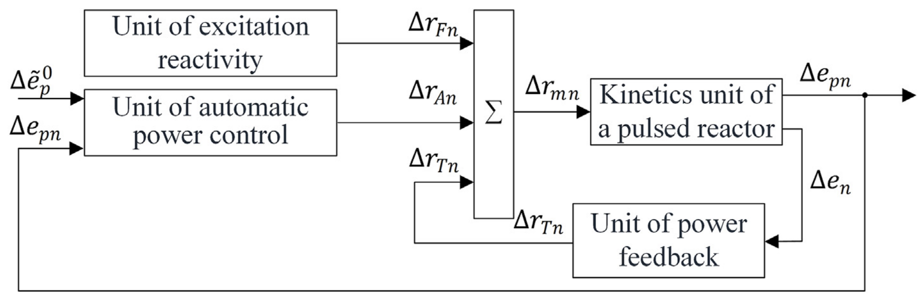

Fig. 3. Block-scheme of model dynamics of the IBR-2M with automatic power control.

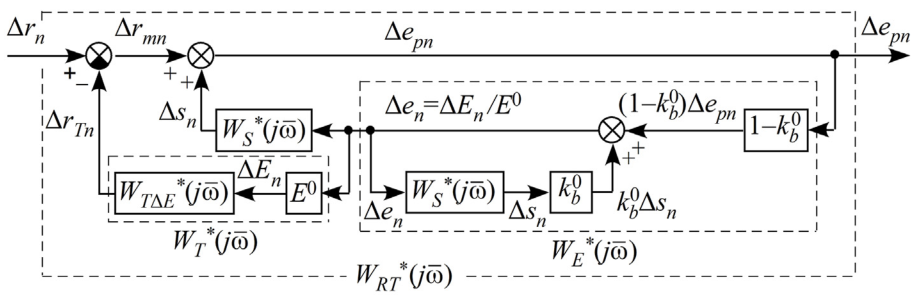

Fig. 4. Structural scheme of the IBR-2M dynamics of non-zero power in a linear approximation in the self-regulation mode: $W_S^*(j\overline{\omega})$, $W_E^*(j\overline{\omega})$ and $W_{T\Delta E}^*(j\overline{\omega})$ – frequency discrete transfer functions.

$$W_S^*(j\overline{\omega})=\frac{\Delta s^*(j\overline{\omega})}{\Delta e^*(j\overline{\omega})}=\frac{1}{\sum_i^6\mu_i\lambda_i\frac{1}{\exp(\lambda_iT_p)-1}}\sum_i^6\mu_i\lambda_i\frac{\exp(-j\overline{\omega})}{\exp(\lambda_iT_p)-\exp(-j\overline{\omega})}$$

$$W_E^*(j\overline{\omega})=\frac{\Delta e^*(j\overline{\omega})}{\Delta e_p^*(j\overline{\omega})}=\frac{1-k_b^0}{1-k_b^0W_S^*(j\overline{\omega})}$$

$$W_{T\Delta E}^*(j\overline{\omega})=\frac{\Delta r_T^*(j\overline{\omega})}{\Delta E^*(j\overline{\omega})}=\sum_j^3\frac{k_{Tj}}{T_{Tj}}\frac{\exp(-j\overline{\omega})}{\exp(T_p/T_{Tj})-\exp(-j\overline{\omega})}$$

$$W_{RTopen}^*(j\overline{\omega})=W_E^*(j\overline{\omega})\left[E^0W_{T\Delta E}^*(j\overline{\omega})-W_S^*(j\overline{\omega})\right] \quad (2)$$

where $W_{RT}^*(j\overline{\omega})$ – the discrete transfer function of the reactor in the self-regulation mode, $\Delta r^*(j\overline{\omega})$ and $\Delta e_p^*(j\overline{\omega})$ – the Fourier transform of discrete signals of reactivity and relative deviation of energy of power pulses, respectively, $W_S^*(j\overline{\omega})$, $W_E^*(j\overline{\omega})$ and $W_{T\Delta E}^*(j\overline{\omega})$ – discrete transfer functions of the delayed neutrons, the kinetics and the power feedback, respectively, E^0 – the basic value of the total energy for the period of power pulses, $\Delta s^*(j\overline{\omega})$ and $\Delta e^*(j\overline{\omega})$ - the Fourier transform of discrete signals of the relative deviation of the intensity of delayed neutrons and the relative deviation of the total energy over the pulse period, T_p – the power pulse period, μ_i and λ_i – the relative fraction and the decay constant of delayed neutrons, respectively, $\Delta r_T^*(j\overline{\omega})$ and $\Delta E^*(j\overline{\omega})$ - the Fourier transform of discrete signals of the power feedback reactivity deviation and the total energy deviation, respectively, k_{Tj} and T_{Tj} – the transfer coefficient and the time constant of j-th PF component ($j = 1, 2, 3$), respectively and $W_{RTopen}^*(j\overline{\omega})$ – the discrete transfer function of an open-loop reactor system in self-regulation mode.

The stability of a closed-loop system (in our case, a self-regulating reactor) can be estimated from the amplitude-phase frequency response (Nyquist plot) of the open-loop system. If the Nyquist plot of an open-loop system does not cover the point with coordinates (– 1, j 0), then the closed-loop system is stable [2,6,7]. The amplitude margin shows by how many times the transfer coefficient of the open part of the system must be increased in order to bring the closed system to the limit of stability, so that the closed system would have continuous oscillations. The phase margin characterizes the allowable increase in signal delay in time. The smaller the phase margin, the closer to instability.

Methods and main results of experiments to estimate parameters of power feedback in the cycle.

The IBR-2M reactor gives the operator a unique opportunity to measure all fast PF components by introducing perturbing reactivity between power pulses (in time less than 0.2 s). The reactor is in a deeply subcritical state between pulses and the introduced reactivity at the moment of power pulse development is perceived as an instantaneous jump. However, because of the large fluctuations in pulse energy (±25%), it is possible to obtain statistically reliable estimates of the amplitudes and timing parameters of all feedback components, up to the shortest, acting within a few pulses (fractions of a second), only when analyzing the transients caused by a sufficiently long series of periodic oscillations of small amplitude reactivity [9]. Periodic modulation of reactivity was performed by moving the AR rod during the time between flashes. The automatic regulator unit in the experiment was used as a perturbing reactivity setter [8]. The energy of each pulse, the position of the automatic regulator and the position of all other regulating units relative to the core, as well as the temperature and sodium flow rate at the entrance to the core were measured to evaluate the PF. Measurements were taken at 1.75, 1.65, 1.55, and 1.50 MW and a sodium flow rate through the core of 100 m^3/h. The interval of total energy output from the beginning of the reactor campaign at the time of measurements was 1400–1700 MW·day.

The fast PF of the IBR-2M can be described as a sum of three parallel links [9]:

$$r_{Tn} = \sum_{j=1}^{3} r_{Tjn}, \quad (3)$$

$$r_{Tjn} = \left(r_{Tjn-1} + \Delta E_{n-1} \frac{k_{Tj}}{T_{Tj}} \right) exp\left(-\frac{T_p}{T_{Tj}} \right), \quad (4)$$

where r_{Tn} and r_{Tjn} are the total reactivity of the PF and its j-th components, corresponding to the n-th power pulse; k_{Tj}, T_{Tj} are the transfer coefficient and time constant of the j-th PF component ($j = 1, 2, 3$), respectively. The PF transfer coefficients were generally assumed to be nonlinear, the $\Delta E_{n-1}-$ deviation of the total energy per period of the nth power pulse from the base value.

Fig. 5 shows, for example, the transient process of pulse energy change at the beginning and end of one of the reactor cycles at 1.75 MW. Table 1 shows the values of the IBR-2M PF parameters corresponding to the transients at the beginning and end of one of the reactor cycles. The value k_T is represented in the so-called pulse delayed neutron fraction β_p per unit change of reactor average power (unit of k_T: β_p/MW). The pulse delayed neutron fraction β_p is allows the known equations of kinetics to be used when the reactor goes into pulse mode [10]. For IBR-2M $\beta_p = 1.54 \cdot 10^{-4}$.

Estimation of stability boundary of the IBR-2M by changing parameters of PF in the cycle.

Since it is necessary to eliminate oscillatory instability in any nuclear-hazardous facilities, let's consider this effect on the IBR-2M in detail. The most informative PF parameter, which depends on power and energy output, is the total transfer coefficient of the fast PF k_T [2]. Fig. 6 shows the change in the total coefficient k_T as a function of the power output in cycles at some power levels. The fast PF limit value $k_T = -2\ \beta_p$/MW in Fig. 6 corresponds to the calculated boundary of oscillatory stability of the reactor in the automatic power regulation mode. In the auto-regulation mode (with the AR system disabled), the reactor is already oscillatively unstable at this value of k_T.

Fig. 6 shows that the total PF coefficient k_T during reactor operation in cycles at 1.75 MW decreases modulo up to the limit of oscillatory stability, but by the beginning of the next cycle takes on average its original value. The change in the coefficient k_T at 1.75 MW, averaged over a set of cycles, can be represented as a linear dependence

$$k_T = (-4,63 \pm 0,19) + (0,15 \pm 0,02)\Delta B,$$

in which k_T is expressed in units of β_p/MW; ΔB is the change in energy output in units of MW·day. Thus, at a power of 1.75 MW, the dependence k_T on the energy output reaches the stability limit already at the energy output equal to 17 MW·day.

The corresponding dependencies obtained at reduced power (1.65 and 1.55 MW) are drastically different from those at 1.75 MW. We can see from Fig. 6 that the dependence k_T at power below 1.75 MW changes weakly with the energy output and has a large margin to the instability boundary. The calculated limits of IBR-2M oscillatory instability in cycles are estimated as follows: at $k_T \le |-2|$ β_p/MW the reactor is unstable in the automatic regulation mode, at $k_T \le |-2.75|$ β_p/MW the instability occurs already in the auto-regulation mode, at $k_T \ge |-4|$ β_p/MW the reactor is always stable.

Additionally, an estimate of the reactor stability boundary from the energy output in the cycle was also obtained using the reactor dynamics model (see Fig. 7). As can be seen from Fig. 7*a*, the amplitude (gain) margin decreases towards the end of the cycle and approaches the so-called zone of unsatisfactory reactor operation equal to three. This boundary is adopted as the recommended maximum allowable for complex systems [11]. The margin equal to one defines the stability boundary in the auto-regulation mode. The phase margin, as can be seen from Fig. 7*b*, is above the maximum allowable value of 35° during the entire reactor cycle, i.e., the reactor is in the phase stability zone in all cycles.

5. Influence of the slow power feedback on the fast ones

In addition to an inner processes of the core that determine the effects of fast PF, slow processes also have a significant effect on feedback reactivity. Here the question arises: can slow reactivity effects affect the value of the fast PF coefficient and, consequently, the reactor dynamics and stability? Let us consider a possible connection between the slow reactivity effects and the fast ones. The slow reactivity was determined by the balance of reactivity. In the critical state, the sum of all reactivity effects is zero [12].

$$\rho_{cr} + \rho_T + \rho_G + \rho_E + \rho_{FP} + \rho_{SP} + \rho_x = 0, \quad (5)$$

where $\rho_{cr} = \sum_{i=1}^{4}[k_i(z_i) - k_i(z_{0i})]$ is the effect of moving control bodies; $k_i(z)$ is the efficiency of the i-th regulation and protection system unit; $\rho_T = k_{temp}(T_{in} - T_{in0})$ is the temperature effect of sodium reactivity at the core inlet (isothermal reactivity effect); T_{in} is the temperature of sodium at the core inlet; k_{temp} - isothermal reactivity factor; ρ_G - reactivity effect of sodium consumption; $\rho_E = k_E(B - B_0)$ - reactivity factor and reactivity effect associated with energy output (fuel burn-up), respectively; $\rho_{FP} = k_P(P - P_0)$, k_P - effect and transfer factor of fast PF, respectively; P - reactor power; ρ_{SP} - slow power feedback effect; ρ_x - other reactivity effects that cannot be accurately estimated numerically, which can be

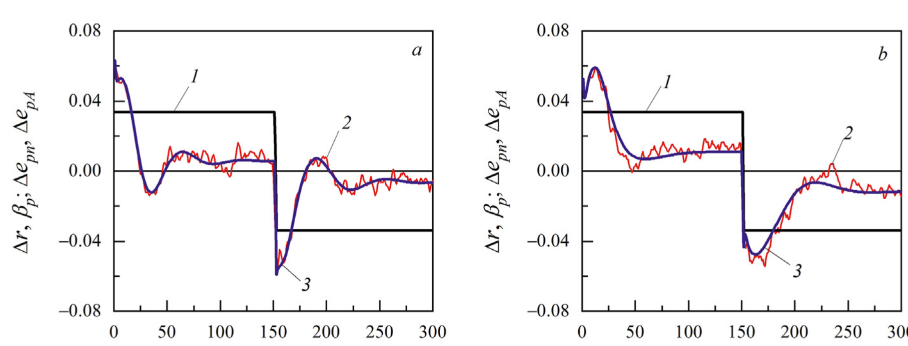

Fig. 5. Transient processes during square oscillation of the driving reactivity $\Delta r = \pm 0{,}034\beta_p$ (*1*) at average power of 1.75 MW in the beginning (*a*) and end (*b*) of reactor cycle: Δe_p, Δe_{pA} − recorded (*2*) and computed (*3*) relative deviation of pulse energy, respectively, n − number of power pulse.

Table 1
Parameters of the fast PF of the IBR-2M at an average power of 1.75 MW and coolant flow through the core of 100 m^3/h in beginning and end of cycle (c_{Tj} – nonlinear coefficient of PF).

Change of energy output from beginning of cycle ΔB, MW•day	Parameter	j – number of PF components		
		1	2	3
3	$k_T = \sum_j k_{Tj}$, β_p/MW	−3.37		
	k_{Tj}, β_p/MW	−3.96	1.24	−0.65
	T_{Tj}, s	8.80	1.31	0.45
	c_{Tj}	0	0	0
16	$k_T = \sum_j k_{Tj}$, β_p/MW	−1.82		
	k_{Tj}, β_p/MW	−1.83	1.95	−1.94
	T_{Tj}, s	11.08	0.59	0.38
	c_{Tj}	0.82	2.03	0.06

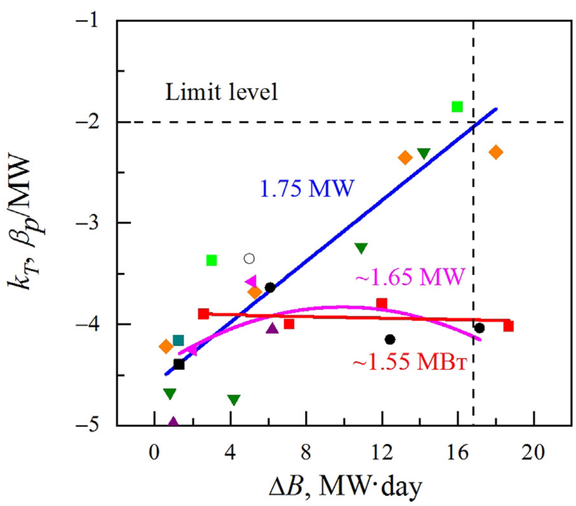

Fig. 6. Dependence of total transfer coefficient PF k_T on energy output ΔB during an certain reactor cycle at average power of 1.75, 1.65 and 1.55 MW. $k_T = -2\ \beta_p$/MW is the calculated stability limit of the IBR-2M reactor in the AR mode.

considered as random noise [12]. The lower index 0 means the parameters corresponding to the impulse criticality state of the given cycle. The temperature and flow feedback coefficients are $k_{temp} = \Delta k/\Delta T = -1.19\cdot 10^{-2}\ \beta_{eff}/°C$ and $k_G = \Delta k/\Delta G = -0.70\cdot 10^{-2}\ \beta_{eff}/m^3/h$, respectively [12,13]. All components in equation (5) are functions of time. The full power feedback ($\rho_P = \rho_{FP} + \rho_{SP}$) can be represented as

$$\rho_P = \sum_{i=1}^{4}[k_i(z_i) - k_i(z_{i0})] - \rho_x - (\rho_T + \rho_G + \rho_E). \quad (6)$$

For the variables included in expression (6), the readings of the research reactor measurement system were used. The period of parameter sampling, except for power, was 0.1 s; for pulse energy, it was determined by the pulse repetition frequency equal to 0.2 s. Fig. 8 shows changes in the total transfer coefficient of the fast PF k_T depending on changes in the slow reactivity and on the position of the IR relative to the core in cycles at different power levels. As can be seen from Fig. 8, the decrease in the k_T coefficient modulo has a clear correlation with the growth of the slow component of the feedback. The physical cause of the slow PF, as shown by studies of this effect on IBR-2 and IBR-2M, is difficult to interpret [12,13]. Here we can only note that each position of the IR unit relative to the core corresponds to a different set of fast PF parameters. For example, as can be seen in Fig. 9, moving the IR downward led to an increase in fast PF and a corresponding decrease in oscillatory instability. Thus, by the end of the reactor cycle, it is possible to change the position of the IR, compensating for the reactivity with another regulator. In addition, for the same purpose, can choose more optimal values for the parameters of the automatic power control system [14].

6. Conclusion

The above data allow us to select the reactor operating modes in which the manifestations of instability are significantly reduced. These measures increase the safety and reliability of the reactor operations. At the same time, it should be noted that the problem of instability of pulse reactors of the IBR-2 type is multidimensional

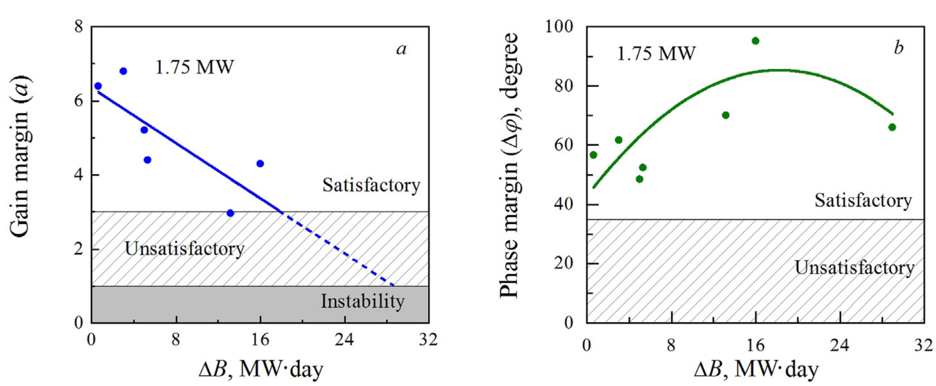

Fig. 7. Estimated changes of stability margins (a – amplitude, b – phase) of the IBR-2M in self-regulating mode dependence on energy output ΔB during the reactor cycle at average power of 1.75 MW.

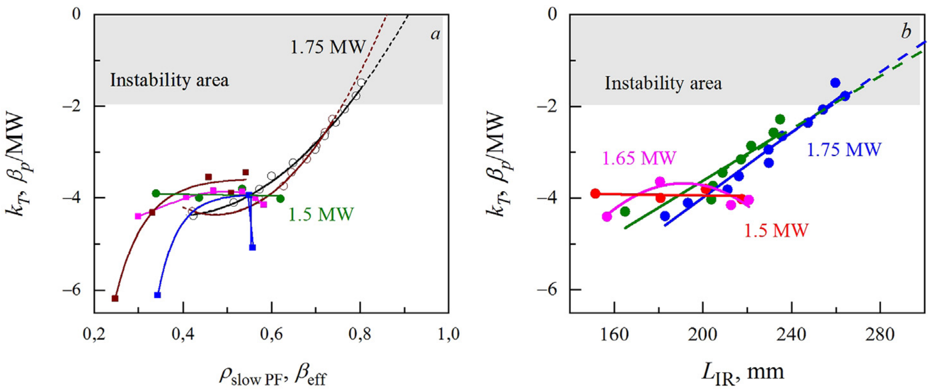

Fig. 8. Change of the total transfer coefficient of the fast PF dependence on slow PF reactivity (*a*) and different position of IR relative to the core in reactor cycle at an average power of 1.75, 1.65 and 1.55 MW (*b*): ■ – L = Var, mm, ■ – L = 200 mm, ■ – L = 100 mm. Gray color indicates the region k_T on the border of the oscillatory instability of the reactor in the AR mode. (For interpretation of the references to color in this figure legend, the reader is referred to the Web version of this article.)

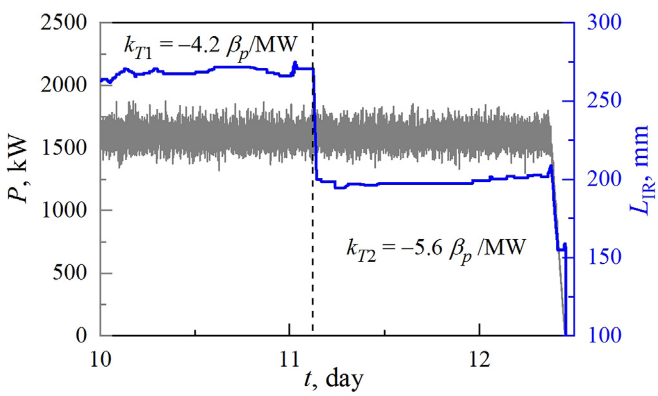

Fig. 9. The effect of amplifying fast PF when moving the IR to a lower position relative to the core at average power of 1.65 MW.

and quite difficult to study. Therefore, the data given in the article are only a fraction of what is needed to understand the nature of the oscillatory instability of the pulse reactor. They do not reveal the physical nature of the oscillatory instability, but only reflect some of its manifestations related to the experimentally observed effect of weakening of the fast PF and its relationship with the slow PF. Further research is needed to investigate the nature of the instability.

Declaration of competing interest

The authors declare that they have no known competing financial interests or personal relationships that could have appeared to influence the work reported in this paper.

Acknowledgements

The authors express their gratitude to the staff of the IBR-2M facility for their help in conducting the experiments.

We thank the “04-4-1105-2011/2022” for support.

References

[1] R.O. Brittan, Analysis of the EBR-1 Core Meltdown (P/2156, USA), vol. 12, Proceedings of the Second United Nations International Conference on the Peaceful Uses of Atomic Energy, Geneva, 1958, pp. 267–272. Reactor physics.

[2] Yu.N. Pepelyshev, A.K. Popov, D. Sumkhuu, et al., On the limits of oscillatory instability of pulsed reactors of periodic operation, Phys. Atom. Nucl. 84 (8) (2021) 77–90, https://doi.org/10.1134/S1063778821080172.

[3] Yu.N. Pepelyshev, A.K. Popov, D. Sumkhuu, Model of the IBR-2M pulsed reactor dynamics for investigating transition processes in a wide range of power variation, Ann. Nucl. Energy 85 (2015) 488–493, https://doi.org/10.1016/j.anucene.2015.06.002.

[4] Yu.N. Pepelyshev, A.K. Popov, D. Sumkhuu, D. Sangaa, Dynamics model of the IBR_2M pulsed reactor for analysis of fast transition processes, Phys. Part. Nucl. Lett. 12 (3) (2015) 435–438, https://doi.org/10.1134/S1547477115030188.

[5] A.A. Marachev, YuN. Pepelyshev, A.K. Popov, D. Sumkhuu, Analysis of dynamics of the IBR-2M reactor with statistically optimal automatic regulator, Atom. Energy 123 (2018) 211–215, https://doi.org/10.1007/s10512-018-0327-3.

[6] Yu.N. Pepelyshev, A.K. Popov, D. Sumkhuu, Stability analysis of the IBR-2M pulsed reactor in automatic regulated regime at various levels of average power, EPJ Web Conf. 173 (2018), 04012, https://doi.org/10.1051/epjconf/201817304012.

[7] Yu.N. Pepelyshev, A.K. Popov, D. Sumkhuu, Investigation of dynamics of the IBR-2M pulsed reactor with energy-production up to 1200 MW·day. J. Phys. Conf., Volume 1391 012099. https://doi.org/10.1088/1742-6596/1391/1/012099.

[8] Y.G. Dragunov, I.T. Tretiyakov, A.V. Lopatkin, et al., Modernization of the IBR-2 pulsed research reactor, Atom. Energy 113 (2012) 29–38, https://doi.org/10.1007/s10512-012-9591-9.

[9] Yu.N. Pepelyshev, A.K. Popov, D. Sumkhuu, IBR-2M reactor power feedback parameters evaluation using square reactivity oscillations, Atom. Energy 122 (2017) 75–80, https://doi.org/10.1007/s10512-017-0238-8.

[10] I.I. Bondarenko, YuYa Stavisskii, Pulsed cycle operation of a fast reactor, Soviet J. Atomic Energy. 7 (1961) 887–890, https://doi.org/10.1007/BF01472391.

[11] Mortimer A. Schultz, Control of Nuclear Reactors and Power Plants, McGraw-Hill book Company, Inc., New York, 1955.

[12] YuN. Pepelyshev, A.D. Rogov, Slow Power Reactivity Feedback Parameters of the IBR-2M Reactor, Communication of JINR, Dubna, 2013.

[13] L.Y. Chan, Y.N. Pepelyshev, Model of IBR-2 power feedback dynamics taking account of slow components, Atom. Energy 104 (2008) 262–267, https://doi.org/10.1007/s10512-008-9026-9.

[14] Yu.N. Pepelyshev, Sumkhuu Davaasuren, Optimization of automatic power control of pulsed reactor IBR-2M in the presence of instability, Nucl. Eng. Technol. 54 (8) (2022) 2877–2882, https://doi.org/10.1016/j.net.2022.03.017.